AAPS PharmSciTech, Vol. 14, No. 3, September 2013 (© 2013)
DOI: 10.1208/s12249-013-9999-0

Research Article

Synthesis of a Smart Gold Nano-vehicle for Liver Specific Drug Delivery

Seema Garg,[1,2] Arnab De,[2] Tanusri Nandi,[1] and Subho Mozumdar[1,3]

Received 15 October 2012; accepted 11 June 2013; published online 9 August 2013

Abstract. Targeting drug formulations to specific tissues and releasing the bioactive content in response to a certain stimuli remains a significant challenge in the field of biomedical science. We have developed a nanovehicle that can be used to deliver "drugs" to "specific" tissues. For this, we have simultaneously modified the surface of the nanovehicle with "drugs" and "tissue-specific ligands". The "tissue-specific ligands" will target the nanovehicle to the correct tissue and release the "drug" of interest in response to specific stimuli. We have synthesised a "lactose surface-modified gold nanovehicle" to target liver cells and release the model fluorescent drug (coumarin derivative) in response to the differential glutathione concentration (between blood plasma and liver cells). Lactose is used as the liver-specific targeting ligand given the abundance of L-galactose receptors in hepatic cells. The coumarin derivative is used as a fluorescent tag as well as a linker for the attachment of various biologically relevant molecules. The model delivery system is compatible with a host of different ligands and hence could be used to target other tissues as well in future. The synthesised nanovehicle was found to be non-toxic to cultured human cell lines even at elevated non-physiological concentrations as high as 100 μg/mL. We discover that the synthesised gold-based nanovehicle shows considerable stability at low extracellular glutathione concentrations; however coumarin is selectively released at high hepatic glutathione concentration.

KEY WORDS: drug delivery; glutathione; gold nanoparticle; spectroscopy; tissue specific.

INTRODUCTION

Nanomedicine is an emerging field that could potentially change the ways we look at and treat various diseases (1). Ideally, drug delivery *via* a well-formulated system should allow release of the "free" drug molecule with improved solubility, *in vivo* stability and appropriate biodistribution (2). However, significant challenges remain which impede the success of clinical trials. Delivering the drug molecule specifically and safely to its target site along with the controlled release of payload are some of the major obstacles that remain to be addressed (3).

We hypothesise that it is possible to simultaneously modify the surface of the nanocarrier with "target bioactive molecules" in addition to "tissue-specific ligands". The system will target the bioactive molecule to the specific tissue receptors. The surface affinity of metallic nanoparticles towards various soft/hard ligands forms the basis of our surface modification approach. Several release strategies have been developed and analysed previously relying either on external (light, electric field, ultrasound, *etc.*) or internal stimuli (pH changes, ionic strength, *etc.*) (4). One such interesting intracellular stimulus is glutathione (tripeptide GSH; the most abundant thiol inside the cells). Its concentration in the blood plasma is 10 μM (5), whereas the intracellular concentration varies from 1 to 10 mM, with the maximum in hepatic cells (6). This 1,000-fold dramatic increase in the concentration makes GSH a promising trigger for intracellular release through place exchange reaction (4). Typically, in abundance of glutathione with respect to other thiols, GSH displaces the existing thiol through the reduction of the linkage that binds the thiol on to the nanoparticles surface rendering the immediate release of the bioactive molecule in the physiological environment.

Previous work has demonstrated the release of a hydrophobic model dye in response to glutathione as a biological stimulus (7). Subsequently (8–15), release of DNA and drug moieties from cross-linked polymeric shells has also been shown. However, following this, not much work has been done in glutathione-mediated release from nanoparticle surface, though it represents one of the most promising triggers for controlled release. Additionally, it remains a big challenge to target the nanoconjugate drug carrier to specific tissues.

By exploiting the fundamentals of gold–thiol chemistry, we have developed a hepatic cell-specific nanodrug delivery vehicle featuring an inert and non-toxic gold core with surface functionalities of thiolated polyethylene glycol (PEG). The PEG moieties are further conjugated with the liver targeting ligand (lactose) and a fluorescent molecule (7-aminocoumarin-3-carboxylic acid) for various biomedical applications. The fluorescent molecule acts as a model to quantify the release of payload in response to variable

Electronic supplementary material The online version of this article (doi:10.1208/s12249-013-9999-0) contains supplementary material, which is available to authorized users.

[1] Department of Chemistry, University of Delhi, Delhi 110007, India.
[2] Department of Microbiology and Immunology, Columbia University Medical Centre, New York, New York 10032, USA.
[3] To whom correspondence should be addressed. (e-mail: subhoscom@yahoo.com)

glutathione concentrations. It also presents an active site for bioconjugation with amine containing drugs and other biomolecules. Another advantage of our model system is that we could potentially change the targeting ligand and target a host of different tissues. Mimicking the *in vivo* conditions, time-dependent *in vitro* release of the model coumarin derivative has been quantified at various glutathione concentrations using fluorescence spectroscopy. The schematic view of the proposed work is shown in Fig. 1.

The gold-based nanovehicle in the current study has been synthesised with the aim of targeting it to the hepatic cells. Diseases associated with liver are largely life-threatening, chronic and lethal. These include hepatocellular carcinoma, hepatitis, liver regeneration, *etc.*, to name a few. All these diseases require a specific therapy and hence specialised therapeutic agents (whose importance as lifesaving agents may surpass the expensive nature of the therapeutic agent). However, the cost of synthesising the nanovehicle has been estimated to be only $1 per mg, a very cost-effective solution. The fact is supported by the existence of various gold-based drug delivery agents, which being simple and cost-effective, are already in the clinical trials with a few being even approved by the US Food Drug Administration (16).

RESULTS AND DISCUSSION

In the present study, we have synthesised the gold nanoparticle-based, hepatic cell-specific, nanovehicle which provides an active site for the conjugation with a variety of bioactive molecules and tissue receptor-specific ligands. The biomolecules could be (containing primary amine functionality) enzymes, drugs, peptides, *etc.* The bioactive is released in response to high glutathione concentrations.

Synthesis of Gold Nanoparticles

Gold nanoparticles were synthesised *via* reverse microemulsion technique which imparted stability, monodispersity and control over the size of the nanoparticles for a prolonged period of time (6 months when stored in micellar template). As

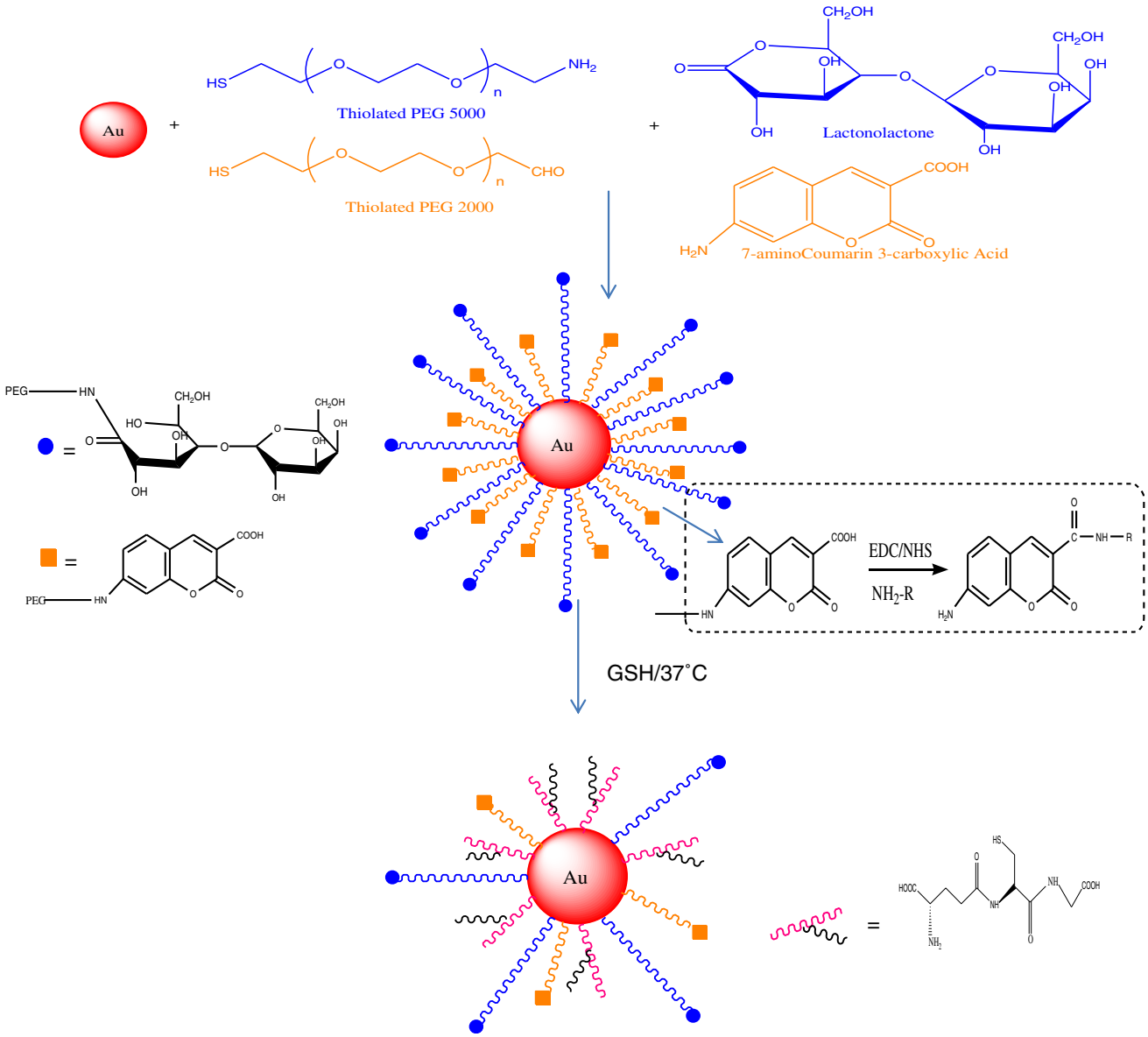

Fig 1. A schematic view of glutathione-mediated release from the surface of liver-specific gold-based nanovehicle

shown by the quasi-elastic light scattering (QELS) data in Fig. 2a, the hydrodynamic radii and dispersity of the nanoparticles in surfactant assemblies remain almost constant over a considerably long period of time with the values of 25± 5 nm and 0.1–0.3, respectively.

Bare gold nanoparticles, extracted out from the surfactant assemblies when needed, also showed a very narrow size range without any signs of pronounced agglomeration (Fig. 2b). Transmission electron microscope (TEM) micrographs of the bare gold nanoparticles show the particles to be uniformly spherical in shape with a size range of about 5–8 nm. These ultra low-sized gold nanoparticles act as efficient core with high surface to volume ratio for further surface functionalization.

Conjugation of PEG Derivatives on the Surface of Bare Gold Nanoparticles

The surface of the gold nanoparticles was modified with thiolated PEG. PEG is used as it is non-immunogenic and has a tendency to act as a soft spacer, imparting flexibility to the system for more efficient interactions with the biological target. The synthesis of the thiolated PEG was carried out in a sequence of steps (Schemes 1, 2, 3, 4, 5 and 6), with apt characterizations done at each step to confirm the chemical synthesis. The synthesised PEG derivatives SH-PEG-NH_2 and SH-PEG-CHO, prior to their coupling with the gold nanoparticles surface, were coupled with target-specific moiety (lactose) and fluorescent linker (7-amino-3-carboxy aminocoumarin), respectively.

Lactose has been employed as the target-specific ligand because liver cells (both Kupffer and parenchymal cells) have receptors on their plasma membranes that specifically bind and internalise ligands with terminal D-galactose residues. Since these receptors are only expressed in the liver, they appear as attractive targets for the specific delivery of bioactive molecules to liver (23). Lactose could be directly conjugated to PEG-NH_2 through reductive amination of its aldehyde group in the presence of sodium cyanoborohydride; however, it was coupled to the thiolated PEG chain in the form of its lactone through ester interchange reaction. This is because the method involving lactose requires a feed ratio of 20–25 equivalents in comparison to 4–8 equivalents for lactonolactone (22). Fourier transform infrared (FTIR) spectra of the coupled product adduct 1 (Fig. S1A) validated successful coupling of the ester (of lactonolactone) with amine (of thiolated PEG) as the peaks for primary amine are absent, instead a prominent broad peak for hydroxyl functionality at 3,400 cm^{-1} (overshadowing the peak for secondary amine at 3,200–3,400 cm^{-1}) is present. N–H bonds are present as weak bands in the region around 1,350 cm^{-1}. In addition, characteristic vibration bands for thiol at 2,910 cm^{-1}, carbonyl group at 1,640 cm^{-1} and C–O bond at 1,108 cm^{-1} are also present.

The fluorescent moiety used for the conjugation is a coumarin derivative. Although coumarin itself is a highly fluorescent molecule, its fluorescence enhances upon derivatization with an electron donating and/or electron withdrawing moiety owing to the extended conjugation of the aromatic system. Hence, instead of coumarin, its 7-amino-3-carboxyl derivative has been employed for the conjugation purpose. Where the amino terminal of the coumarin derivative behaved as a flexible

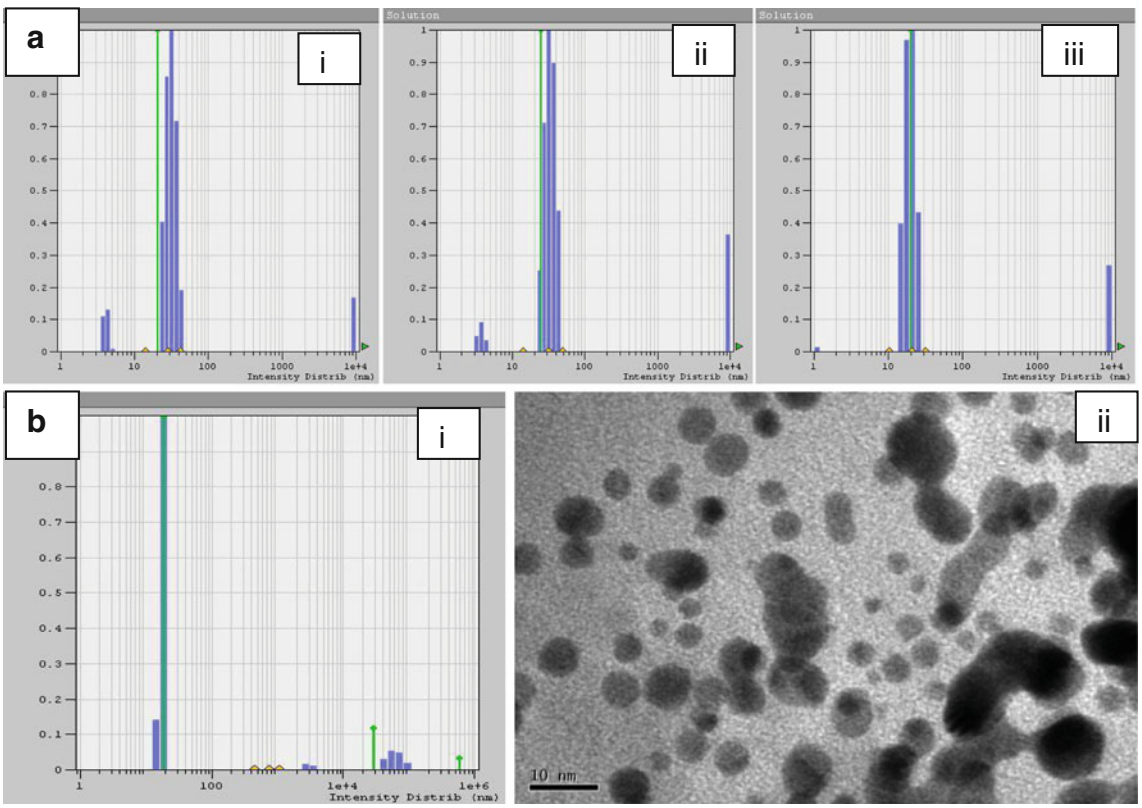

Fig 2. **a** QELS data showing the hydrodynamic radii of surfactant-protected gold nanoparticles stored in reverse micelle template. (*i*) At 1 day after synthesis, (*ii*) at a month after synthesis, (*iii*) at 3 months after synthesis. **b** Characterization data of bare gold nanoparticles (*i*) QELS data showing size distribution in water, (*ii*) TEM micrograph at scale of 10 nm

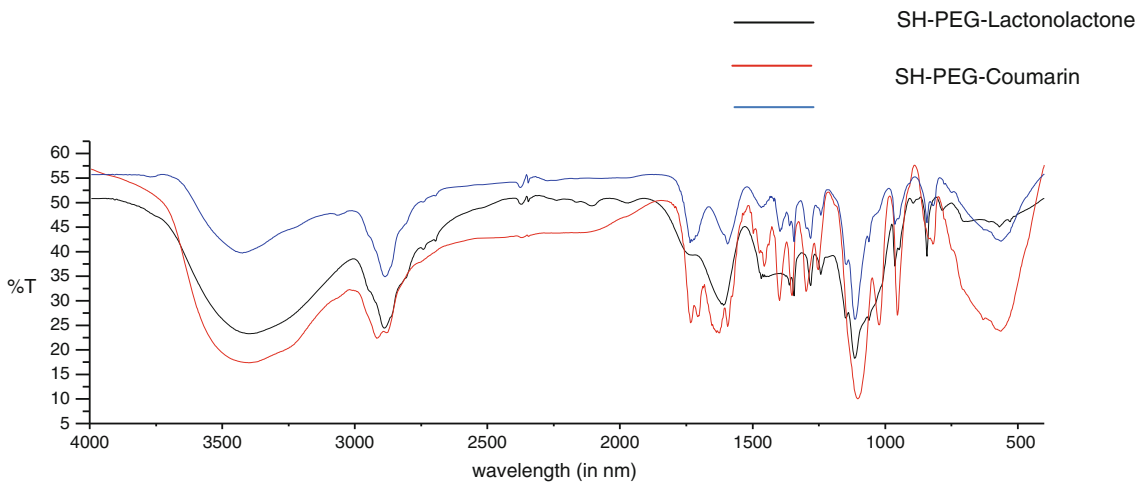

Fig. 3. An overlay of the FTIR spectra of adduct 1, adduct 2, and conjugated gold nanoparticles

arm for coupling with SH-PEG (2000)-CHO, its carboxyl terminal presents an active centre for the attachment of a variety of biologically relevant molecules, both covalently and non-covalently.

The coupling of 7-aminocoumarin-3-carboxylic acid with PEG-CHO involves a simple Schiff's base formation reaction followed by the reductive amination with sodium cyanoborohydride ($NaCNBH_3$). The formation of the coupled product (adduct 2) has been analysed through FTIR, nuclear magnetic resonance (NMR) and UV–vis spectroscopy. The FTIR spectrum of the coupled product (Fig. S1B) shows characteristic peaks around 3,400 and 2,910 cm^{-1} attributed to the vibrational stretching of carboxyl group (outshining the peak for secondary amine) and thiol functionality, respectively. Presence of the signature vibration bands for carbonyl group of both acid and ester at 1,710 and 1,735 cm^{-1} and C–O at 1,110 cm^{-1} authenticates the coupling reaction. In addition, the fingerprint region in the FTIR spectrum clearly highlighted the aromaticity in the coupled product. The NMR spectra also show signals for secondary amine and thiol functionality in the range of δ 0.8–1.5 ppm. Signals for aromaticity in the range of δ7.0–8.0 ppm were also observed (Fig. S2). UV–vis analysis also revealed a hypsochromic shift in the λ_{max} value from 373 nm for 7-aminocoumarin 3-carboxylic acid to 368 nm for PEG-conjugated coumarin as shown in Fig. S3. All these characteristic data confirmed the successful coupling of the thiolated PEG chains 5,000 and 2,000 with the target-specific and fluorescent moiety, respectively.

The final conjugation of the coupled PEG derivatives with gold nanoparticles was carried out at physiological pH. An overlay of the FTIR spectra of the conjugated gold nanoparticles (Fig. 3) with adduct 1, SH-PEG-lactonolactone and adduct 2, and SH-PEG-coumarin clearly shows the successful conjugation reaction. The FTIR spectrum of conjugated gold nanoparticles shows a broad peak at 3,400 cm^{-1} fusing the peaks for OH, COOH and N–H stretch. In addition, characteristic vibration bands for C–O stretch at 1,100 cm^{-1} and for carbonyl functionalities around 1,650 cm^{-1} are also present in comparison to absence of any such peaks in the FTIR spectra of bare gold nanoparticle (Fig. S4). The shift in the λ_{max} value of the bare gold nanoparticle upon conjugation with PEG derivatives was also analysed. Figure S5 demonstrates a bathochromic shift in the absorption wavelength of gold nanoparticles from 522 to 551 nm upon conjugation with thiolated PEG derivatives. Size distribution plots (QELS data) and TEM micrographs (Fig. S6) also point towards an increase in the size of the nanoparticle to 20–30 nm after conjugation. It was also found that the fluorescence of the coumarin, covalently attached to PEG (2000) derivatives, got quenched in the conjugated product as gold nanoparticles behave as efficient fluorescence quenchers (Fig. 4).

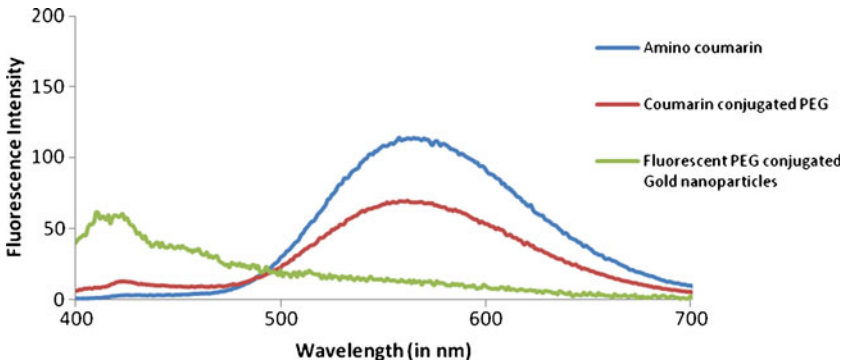

Fig. 4. Fluorescence spectra showing quenching of fluorescence by gold nanoparticles

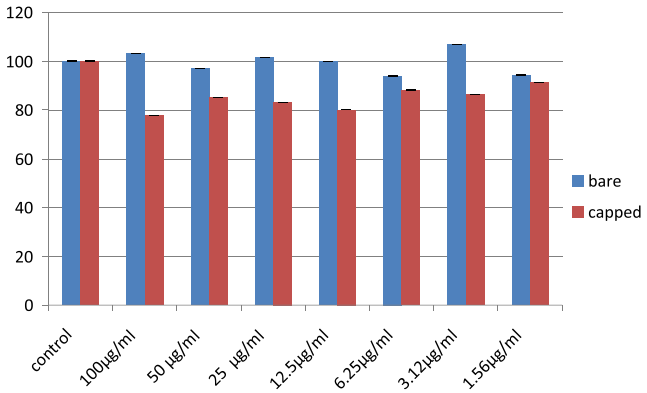

Fig. 5. A comparative analysis of the percentage cell viability of A549 cells at variable concentration of bare and conjugated gold nanoparticles

In Vitro Cytotoxicity Assessment of Conjugated Gold Nanoparticles

Samples of conjugated gold nanoparticles and bare gold nanoparticles were assessed for their concentration-dependent cytotoxicity on cultured A549 cell lines *via* 3-(4,5-dimethylthiazol-2-yl)-2,5-diphenyltetrazolium bromide (MTT) cytotoxicity assay. The concentrations of the gold samples varied from 100 to 1.56 µg/mL, prepared *via* the serial dilution of the stock at 100 µg/mL. The results were recorded in triplicates, analysed and have been graphically presented as a comparative plot of percentage cell viability after 24 h of incubation with bare and conjugated gold nanoparticles separately *vs.* concentration of the gold samples in Fig. 5.

As observed individually for bare and conjugated gold nanoparticles, results for the percentage cell viability of treated A549cells with reference to the control indicated that the cells were viable at all the concentrations of the samples ranging from 100 to 1.56 µg/mL. The cells showed an average percentage cell viability of 95% and above for bare gold nanoparticles and 80% and above for conjugated gold nanoparticles, respectively, at all the concentrations.

However, on comparing the toxicity of the two different gold samples at variable concentrations, it has been found that practically at all the concentrations, the average percentage cell viability of the A549 cells decreased for the cells incubated with conjugated gold nanoparticles than those incubated with bare gold nanoparticles. That is to say that the surface functionalization of the bare gold nanoparticles with thiolated PEG derivatives imparted slight incompatibility in the gold nanoparticles though not to the toxic and risky levels as even after functionalization, an average percentage cell viability of 80% and above is observed at almost all the concentrations. It has also been observed that with a decrease in the concentration of the conjugated gold nanoparticles, a corresponding increase in the percentage cell viability occurred thereby rendering the nanovehicle completely biocompatible at biologically relevant dosages ranging from 6.25 to 1.56 µg/mL.

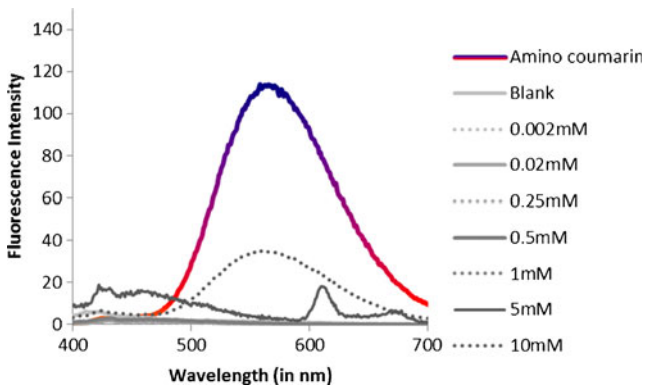

Fig. 6. Fluorescence spectra showing release of fluorescent moiety at variable glutathione concentration

Glutathione-Mediated *In Vitro* Release Studies

Since gold nanoparticles serve as excellent fluorescent quenchers (24), they allow the *in vitro* release of aminocoumarin from nanoparticle's surface to be observed by fluorescence spectroscopy. For the release studies, functionalized gold nanoparticles were incubated with different concentration of glutathione starting from 2.5 to 10 mM at physiological temperature for a time span of 6 h. A blank study involving the incubation of the gold nanoparticles with PBS buffer without glutathione was also performed. The release of fluorescent coumarin derivative was then quantified as a function of both time and glutathione concentration.

The release of aminocoumarin as a function of glutathione concentration is shown in Fig. 6. The result indicates that fluorescence of coumarin (covalently attached to the thiolated PEG adhered over nanoparticle surface) remains quenched till glutathione concentration of 1 mM (and lower); however, at the glutathione concentration of 5 mM, a peak with signal intensity of 20 was observed and the signal intensity enhanced to 35 with the increasing concentration of glutathione up to 10 mM. This phenomenon can be explained on the basis of place exchange reaction of glutathione with the thiols on gold nanoparticle surface (8,9). At low concentrations of glutathione (≤1.0 mM), the biological thiol is either not sufficient enough to displace the thiols on the nanoparticle surface or else the thiols on the nanoparticle surface are in more concentration than glutathione thereby shifting the equilibrium towards conjugation of nanoparticles with thiolated PEG. However, as the concentration increases to 10 mM, glutathione act as trigger to displace thiolated PEG from the nanoparticle surface. As the thiolated PEG disassembled from the nanoparticle surface, the influence of the later on the fluorescence characteristics of coumarin derivative disappeared resulting in a sharp signal peak in its respective fluorescence spectrum. In contrast to these nanoparticles (incubated in glutathione solution), the particles incubated with buffer only did not show any release of the fluorescent moiety thereby highlighting the role of glutathione at a particular concentration as the release trigger for payload through thiol place exchange reaction. Hence, we conclude that the synthesised nanovehicle if applied *in vivo* would remain stable extracellularly, where the glutathione concentration is 10 µM; however, after internalisation it would show considerable release inside the hepatic cells.

The influence of time on *in vitro* release behaviour of aminocoumarin from the nanoparticle surface was also analysed. The nanoparticles incubated with buffer did not show any release with subsequent fluorescence for 24 h, but the nanoparticles incubated with 10 mM of glutathione

(equivalent to glutathione concentration in liver cells) showed a gradual increase in the fluorescence intensity reaching a maximum in 2.5 h. Time-dependent release of the nanoparticles incubated with 10 μM of glutathione was also analysed. It showed negligible release even after 24 h of incubation at physiological temperature. Figure 7 depicts the time-dependent glutathione-mediated release of aminocoumarin from the nanoparticle surface. The r^2 value as determined for the time-dependent release for nanoparticles incubated at 10 mM was found to be 0.99 indicating a gradual release w.r.t time.

Since glutathione-mediated *in vitro* release of the payload has been analysed and interpreted mimicking most of the *in vivo* conditions, it can be easily said that the synthesised nanovehicle might be useful for various liver-targeted drug delivery applications by just attaching the bioactive molecule to the fluorescent moiety *via* carbodiimide chemistry. In general, as mentioned above, most of the liver-associated diseases are life-threatening, chronic and lethal with a few examples being hepatocellular carcinoma, hepatitis, *etc.* The drugs used for the therapy of these diseases could be easily conjugated to the nanovehicle through the carboxyl end of the fluorescent linker employing EDC-NHS chemistry. The release of the drug in turn is achieved through lysis of the pH labile bond between the bioactive molecule and carboxycoumarin at endosomal/lysosomal pH inside the cell. Since the synthesised nanovehicle would target only the liver tissue, the side effects of the drugs, as observed in the case of nonspecific drug targeting, are minimised to considerable levels with a corresponding increase in their therapeutic efficacy.

EXPERIMENTAL PROCEDURE

Materials

All starting materials were purchased from commercial sources and were used without further purification. Specifically, gold chloride (49–50% Au), methoxy PEG 2000 (polyethylene glycol) and methoxy PEG 5000 were procured from Sigma-Aldrich. Both monomethoxy PEG products were azeotropically refluxed with toluene so as to remove the excess water prior to their usage. All solvents and salts of analytical grade were obtained from Merck. Salicylaldehyde, malonic acid, tosyl chloride, lithium aluminium hydride, potassium thioacetate, sodium azide and tin chloride were products of Aldrich Chemicals. Acids used during the experimentation were obtained from Fischer Scientifics.

Air- or/and moisture-sensitive reactions were carried out under argon or nitrogen atmosphere. ^{1}H spectra were recorded on a Bruker Advance_ AC-400 instrument at 400 MHz. Chemical shifts were measured relative to that of $CDCl_3$ (d 7.26) and DMSO-d_6 and are expressed in parts per million. The following abbreviations are used to describe the signal multiplicities: s (singlet), br s (broad singlet), d (doublet), t (triplet), q (quartet) and m (multiplet). FTIR spectra (400–4,000 cm^{-1}) were recorded using NaCl discs on a PerkinElmer instrument. TEM analysis was performed on a Technai F2 instrument at a voltage of 300 MV.

Fluorescence studies were conducted on a CARY instrument with an excitation value of 380 nm. The dynamic light scattering measurements for estimating the average mean size and polydispersity index for the synthesised nanoparticles was obtained from a Photocor FC instrument having Argon ion laser (633 nm) as the light source and Dyna LS as the software for accumulating data points and plotting a diffractogram. UV–vis analysis for the samples was done on Double beam Systronics AU2700 instrument

Synthesis of Gold Nanoparticles

Gold nanoparticles were synthesised employing the reverse microemulsion approach using a biocompatible nonionic surfactant as the amphiphile, cyclohexane as the continuous phase and aqueous salt solutions as the dispersed phase. Briefly, microemulsion A was prepared by adding 180 μL of 0.05 M gold chloride to 25 mL of stock surfactant solution, whereas microemulsion B was prepared by adding 180 μL of 0.25 M $NaBH_4$ to a separate 25 mL of stock surfactant solution. Both the microemulsions were equilibrated under constant magnetic stirring for 45 min before microemulsion B was mixed to microemulsion A to form a homogeneous microemulsion mixture (microemulsion C). The resultant microemulsion was left on stirring for 4–5 h. The physicochemical analysis of the surfactant-protected nanoparticles was done using various characterization techniques and the nanoparticles were stored in the same form so as to avoid

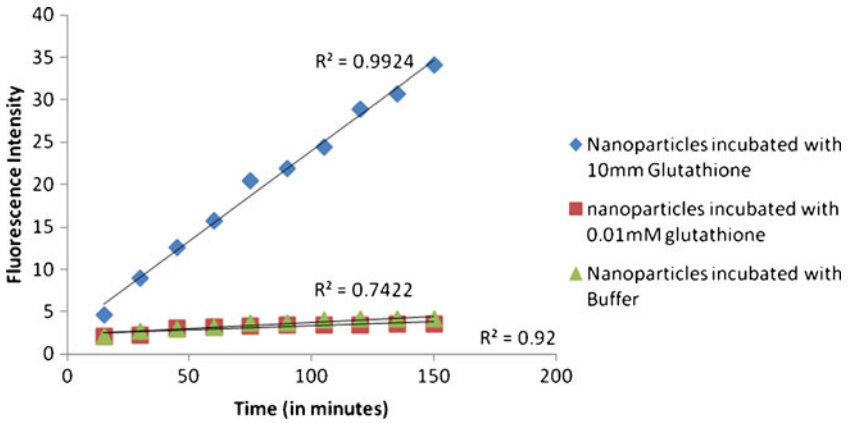

Fig. 7. Fluorescence spectra showing time-dependent release of fluorescent moiety in buffer and at glutathione concentration of 10 μM and 10 mM

aggregation and agglomeration phenomenon and efficient usage in the later stages of experimentation.

Synthesis of Lactonolactone, 7-Aminocoumarin 3-Carboxylic Acid and Functionalized PEG

The syntheses is described in the Supplemental Methods section (Schemes S1, S2, S3 and S4)

Coupling of Lactonolactone to SH-PEG-NH_2[22]

The coupling reaction of the lactonolactone (8.0 Eq) with SH-PEG-NH_2 (1.0 eq) was carried out in DMF at 100°C for 30 h under inert atmosphere (Scheme S5). The progress of the reaction was monitored through TLC ($CHCl_3$/MeOH system) so as to ensure that unreactive lactonolactone was not contained in the product formed. After the completion of the reaction, the final product was sequentially precipitated out formerly with MEOH/dry ether (1:1) mixture and finally with dry ether. The product when dried under vacuum overnight gave brown coloured solid (adduct 1).

Coupling of 7-Aminocoumarin 3-Carboxylic Acid to SH-PEG-CHO

Coumarin derivative (1.0 eq) was dissolved in minimum amount of methanol and few drops of triethylamine were added to it so as to adjust the pH to 8.0 (Scheme S6). To this stirring solution, 4 equivalents of aldehyde and 25 μL of 5 M sodium cyanoborohydride were added under inert atmosphere. The reaction mixture was left on stirring overnight at room temperature maintaining the inertness of the system. The progress of the reaction was monitored through TLC ($CHCl_3$/MeOH) so as to ensure the absence of unreacted coumarin derivative from the adduct. After the completion of the reaction, the solvent was evaporated and the solid was treated with CH_2Cl_2. The solution was filtered to remove the unreacted excessive reagents. Purification by silica chromatography (CH_2Cl_2/MeOH) yielded the final product as a bright yellow-coloured solid (adduct 2).

Conjugation of Adduct 1 and Adduct 2 with Gold Nanoparticles

Prior to coupling, the surfactant-protected Gold nanoparticles were treated with benzene/methanol (3:1) mixture so as to disrupt the surfactant assemblies and extract out the bare gold nanoparticles from them. The extracted nanoparticles were collected, washed and dispersed in 5 mL of phosphate buffer at pH 7.4. Separately, adduct 1 and adduct 2 were also dispersed in 2 mL of the PBS buffer at pH 7.4. Under inert conditions, 500 μL of adducts 1 and 2 was added to 5 mL of the gold colloid solution followed by the incubation at room temperature for 24 h maintaining the inertness of the system. The colloidal suspension was then centrifuged to separate out the functionalized nanoparticles. The nanoparticles were washed extensively with ethanol. Finally, the washed nanoparticles were re-dispersed in 5 mL of the phosphate buffer (pH 7.4).

In Vitro Cytotoxicity Assessment of Conjugated Gold Nanoparticles

The cytocompatibility studies of the surface functionalized and bare gold nanoparticles were carried out on A549 human cell lines *via* MTT cell viability assay. Human alveolar basal epithelial (A549) cells were cultured in Dulbecco's modified Eagle's medium supplemented with 10% foetal bovine serum (Invitrogen) and 1% antibiotic (Sigma). The cells were maintained at 37°C in a 5% CO_2 incubator. Approximately, 1×10^5 cells were plated in 96 well plates. Various concentrations of the bare and conjugated gold nanoparticles were then prepared *via* serial dilution method from a stock solution of 100 μg/mL. The concentrations of the gold samples so obtained were 100, 50, 25, 12.5, 6.25, 3.125 and 1.56 μg/mL. Each concentration was assessed in triplicate. That is to say that each concentration of the bare and conjugated gold nanoparticles was added in triplicates to the A549 cells in 96 well plate. After adding the gold samples, the cells were incubated at 37°C in 5% CO_2 incubator for 24 h. After incubation, 20 μL of MTT reagent (Sigma) was added to each well and was again incubated for 3 h at 37°C. Following this, the MTT reagent was removed and 100 μL of DMSO (solubilisation solution) was added in each well. The plate was then kept for vigorous shaking for about 15 min with the subsequent measurement of the optical density (of cells) at 570 nm.

Glutathione-Mediated *In Vitro* Release Studies

Varied concentrations of reduced glutathione were prepared in PBS buffer ranging from 2.5 μM to 10 mM and were checked for their UV absorption and fluorescence values. Then separately, to a 3-mL aliquot of the glutathione solution at all the prepared concentrations maintained at 37°C, 500 μL of bioconjugated gold colloid in PBS buffer was added. The resulting colloid was incubated for 6 h at 37°C and the release of fluorescent moiety from the gold surface was quantified as a function of variable glutathione concentration and time.

CONCLUSION

Various delivery systems have been designed in the past for modulated delivery of active drugs (25,26). A glutathione-mediated hepatic cell-specific drug delivery vehicle has been synthesised featuring a non-toxic gold core, PEG as the soft spacer, lactose as the target-specific moiety and 7-aminocoumarin 3-carboxylic acid as the bioactive fluorescent moiety. The fluorescent moiety can serve both as a linker for bioconjugation with molecules of biological importance and as a model to quantify the release through fluorescence spectroscopy. Cytotoxicity assessment of the nanovehicle on cultured human cell lines reveals its possible administration inside the body up to concentrations as high as 100 μg/mL. *In vitro* time-dependent release of the fluorescent molecule has been quantified as a function of variable glutathione concentration and it has been found that the nanovehicle releases its content at the glutathione concentration of 5–10 mM (as inside the hepatic cells) within 2.5 h of its administration. However, the nanovehicle is stable at glutathione concentrations of 10 μM as present extracellularly. Thus, we show that by tuning the

surface properties for convenient delivery parameters, the synthesised system would act as an efficient glutathione-mediated drug delivery vehicle to hepatic cell lines. By changing the biomolecule and the target-specific ligand, it is possible to use our system to carry other drugs to a host of different tissues.

ACKNOWLEDGMENTS

The authors thank the Department of Science and Technology for the financial assistance in the form of Junior Research Fellowship and the University Science Instrumentation Centre, University of Delhi, for providing the characterization facilities.

REFERENCES

1. Khademhosseini A, Langer R. Applications in drug delivery and tissue engineering nanobiotechnology. SBE. 2006;102:38–42.
2. Ghosh P, Han G, De M, Kim CK, Rotello VM. Gold nanoparticles in delivery applications. Adv Drug Deliv Rev. 2008;60:1307–15.
3. Mishra B, Patel BB, Tiwari S. Colloidal nanocarriers: a review on formulation technology, types and applications toward targeted drug delivery. Nanomedicine: Nanotechnol Biol Med. 2010;6:9–24.
4. Chompoosor A, Han G, Rotello VM. Charge dependence of ligand release and monolayer stability of gold nanoparticles by biogenic thiols. Bioconjug Chem. 2008;19:1342–5.
5. Jones DP, Carlson JL, Mody Jr VC, Cai J, Lynn MJ, Sternberg Jr P. Redox state of glutathione in human plasma. Free Radic Biol Med. 2000;28:625–35.
6. Anderson ME. Glutathione: an overview of biosynthesis and modulation. Chem Biol Interact. 1998;111:1–14.
7. Hong R, Han G, Fernández JM, Kim B, Forbes NS, Rotello VM. Glutathione-mediated delivery and release using monolayer protected nanoparticle carriers. J Am Chem Soc. 2006;128:1078–9.
8. Han G, Chari NS, Verma A, Hong R, Martin CT, Rotello VM. Controlled recovery of the transcription of nanoparticle-bound DNA by intracellular concentrations of glutathione. Bioconjug Chem. 2005;16:1356–9.
9. Liu J, Pang Y, Huang W, Huang X, Meng L, Zhu X, *et al*. Bioreducible micelles self-assembled from amphiphilic hyperbranched multiarm copolymer for glutathione-mediated intracellular drug delivery. Biomacromolecules. 2011;12:1567–77.
10. Cai XJ, Dong HQ, Xia WJ, Wen HY, Li XQ, Yu JH, *et al*. Glutathione-mediated shedding of PEG layers based on disulfide-linked catiomers for DNA delivery. J Mater Chem. 2011;21:14639–45.
11. Wen HY, Dong HQ, Xie W, Li YY, Wang K, Pauletti GM, *et al*. Rapidly disassembling nanomicelles with disulfide-linked PEG shells for glutathione-mediated intracellular drug delivery. Chem Commun. 2011;47:3550–2.
12. Tang LY, Wang YC, Li Y, Du JZ, Wang J. Shell-detachable micelles based on disulfide-linked block copolymer as potential carrier for intracellular drug delivery. Bioconjug Chem. 2009;20:1095–9.
13. Li D, Li G, Guo W, Li P, Wang E, Wang J. Glutathione-mediated release of functional plasmid DNA from positively charged quantum dots. Biomaterials. 2008;29:2776–82.
14. Koo AN, Lee HJ, Kim SE, Chang JH, Park C, Kim C, Park JH, Lee SC. Disulfide-cross-linked PEG-poly(amino acid)s copolymer micelles for glutathione-mediated intracellular drug delivery. Chem Commun (Camb). 2008; 6570–72.
15. Navath RS, Kurtoglu YE, Wang B, Kannan S, Romero R, Kannan RM. Dendrimer–drug conjugates for tailored intracellular drug release based on glutathione levels. Bioconjug Chem. 2008;19:2446–55.
16. Kumar A, Zhang X, Liang X-J. Gold nanoparticles: emerging paradigm for targeted drug delivery system. Biotechnol Adv. 2013;31:593–606.
17. Kobayashi K, Sumitomo H, Ina Y. Synthesis and functions of polystyrene derivatives having pendant oligosaccharides. Polym J. 1985;17:567–75.
18. Besson T, Coudert G, Guillaumet G. Synthesis and fluorescent properties of some heterobifunctional and rigidized 7-aminocoumarins. J Heterocycl Chem. 1991;28:1517–23.
19. Stefanko MJ, Gun'ko YK, Rai DK, Evans P. Synthesis of functionalised polyethylene glycol derivatives of naproxen for biomedical applications. Tetrahedron. 2008;64:10132–9.
20. Shenoy D, Fu W, Li J, Crasto C, Jones G, DiMarzio C, *et al*. Surface functionalization of gold nanoparticles using hetero-bifunctional poly (ethylene glycol) spacer for intracellular tracking and delivery. Int J Nanomedicine. 2006;1:51.
21. Ladd DL, Henrichs PM. Synthesis and NMR characterization of monomethoxypoly(ethylene glycol) aldehydes from monomethoxypoly(ethylene glycol) tosylates. Synth Commun. 1998;28:4143–9.
22. Ouchi T, Uchida T, Arimura H, Ohya Y. Synthesis of poly (L-lactide) end-capped with lactose residue. Biomacromolecules. 2003;4:477–80.
23. Bijsterbosch MK, Van Berkel T. Uptake of lactosylated low-density lipoprotein by galactose-specific receptors in rat liver. Biochem J. 1990;270:233.
24. Dulkeith E, Morteani A, Niedereichholz T, Klar T, Feldmann J, Levi S, *et al*. Fluorescence quenching of dye molecules near gold nanoparticles: radiative and nonradiative effects. Phys Rev Lett. 2002;89:203002.
25. De A, DiMarchi RD. Investigation of the feasibily of an amide-based prodrug under physiological conditions. Int J Pept Res Ther. 2008;3:255–62.
26. De A, DiMarchi RD. Synthesis and characterization of ester-based prodrugs of glucagon-like peptide 1. Pept Sci. 2010;94(4):448–56.